Finite-Size Effects: Hydrogen in Fe/V(001) Superlattices

Xiao Xin, Gunnar K. Pálsson, Max Wolff,* and Björgvin Hjörvarsson
Division of Materials Physics, Department of Physics and Astronomy, Uppsala University, Box 516, S-75120 Uppsala, Sweden
(Received 25 November 2013; published 23 July 2014)

We investigate the effect of finite size on phase boundaries of hydride formation in ultrathin metallic films, using Fe/V(001) superlattices as a model system. The critical temperature is determined to scale linearly with the inverse thickness of the V layers. The decrease of the ordering temperature with decreasing layer thickness arises from the missing H neighbors at the interfaces, analogous to observed finite-size effects in magnetic layers and nanosized ice crystals.

DOI: 10.1103/PhysRevLett.113.046103 PACS numbers: 68.55.Ln, 64.60.an, 77.55.Px, 78.66.Bz

The physical properties of condensed matter can be affected by the actual size of the material, for instance when the size is comparable to the interatomic distances. Investigations of finite-size and interface effects can, e.g., be performed by sandwiching a ferromagnetic layer between paramagnetic materials. This approach has been used to investigate the effect of finite size on the magnetic ordering temperature (in thin films) [1,2], the influence of boundaries on the magnetic ordering [3], and the influence of exchange coupling on ordering in magnetic superlattices [4]. Finite-size and boundary effects are not restricted to man-made materials. Strong effects are seen in the nucleation of ice [5] and the effect of the air-ice boundaries can even be experienced in everyday life through the low friction encountered when skating. The early scientific debate on the friction of ice was based upon the known bulk properties and a pressure or heat induced melting of the near surface layer. This view was later rejected and profound boundary effects emerged as the correct description: A near surface region of a liquidlike state is formed, even at temperatures well below freezing [6,7]. Hydrogen absorbed into certain metals has a phase diagram that is topologically similar to a fluid [8]. The H-H interaction is of long range, which makes the thermodynamic properties highly susceptible to finite-size effects [8–10]. The effect of finite size is, for example, seen in the shift of the phase boundaries and/or a narrowed miscibility gap [11] and studies of Nb grown on Al_2O_3 [12,13] substrates demonstrated substantial changes in the critical temperature with thicknesses of the Nb layers.

Reversible charging and uncharging at moderate temperatures together with a high gravimetric density is required for the utilization of hydrogen as an energy carrier. Tuning the absorption potential in metal hydrides, complex hydrides, and porous materials by finite-size effects has been suggested as a route to achieving this goal [10]. The most recent efforts focus on confinement and the influence of micro- and nanostructures to tune the kinetic and thermodynamic properties of metal hydrides [13–20]. This approach complements the search for new complex [21,22] and intermetallic hydrides [23], where the hydrogen absorption properties are mainly related to the electronic structure [24].

In this Letter we quantify the finite-size dependence of the order-disorder phase transition of hydrogen in ultrathin metallic vanadium (001) layers. The ordered V_2H phase has a lower density than the disordered state, resembling the density differences of water and ice. We will show that the results are general by comparing them to magnetic phase transitions and emphasizing the similarities with the water-ice phase diagram. The results show that finite-size effects only become prominent on the nanometer length scale, which has strong implications on the applicability of the approach for hydrogen storage.

Transition metals can be viewed as the archetype for interstitial hydrides [25–27]. We therefore chose to use single crystal vanadium (001) layers confined by iron (001) in Fe/V(001) superlattices for exploring the effect of confinement on hydrogen uptake. The hydrogen absorption is exothermic in V (−0.3 eV/H atom [28]) while it is endothermic in Fe (+0.3 eV/H atom [29]). As a result, hydrogen is absorbed exclusively in the V layers. The low concentration (smaller than 0.07 H/M) phase (α phase) is characterized by tetrahedral occupancy (see Fig. 1) of the hydrogen while the hydrogen occupies octahedral sites in the ordered β phase. For a thorough description of the bulk vanadium phase diagram, see Ref. [27]. The strain state of the absorbing material also needs to be included due to profound influence on the hydrogen uptake [30–32]. In Fe/V(001) superlattices, the V(001) is under a biaxial compressive strain, making the octahedral z sites more favorable for hydrogen occupancy, even at low hydrogen concentrations. As a consequence, the site occupancy of H in Fe/V(001) resembles that of the bulk β phase [33]. As a consequence, the disorder to order phase transition of H in Fe/V(001) superlattices takes place without a change in hydrogen site occupancy. Fluctuations in the hydrogen density near the critical point are therefore possible [34], in stark contrast to unstrained bulk [26]. The critical temperature of the disorder to order transition of H can, therefore, be used to determine the influence of confinement on the ordering, as described below.

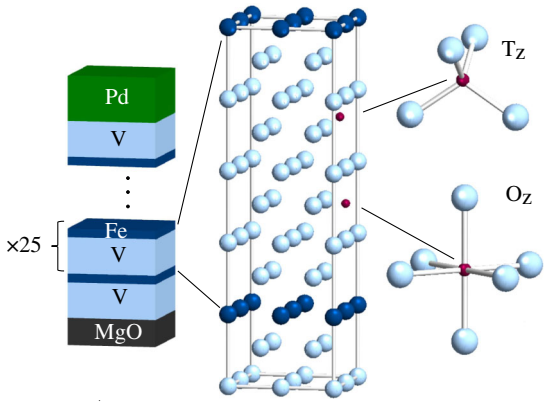

FIG. 1 (color online). Sketch of the sample design. 25 bilayers of Fe/V(001) are grown as a single crystal on a MgO substrate, with a Pd capping protecting against oxidation and catalyzing the hydrogen uptake. The panels on the right-hand side show two types of interstitial sites that hydrogen (red spheres) can occupy: O_z (octahedral z site) and T_z (tetrahedral z site). Light blue and dark blue spheres symbolize the V atoms and the Fe atoms, respectively.

The benefits of using a metallic superlattice is twofold: The sample quality can easily be determined using x-ray scattering techniques [35] and the use of many repeats improves the accuracy of the experiments. The Fe/V superlattices were grown epitaxially on a $10 \times 10 \times 0.5$ mm^3 MgO(001) single-crystal substrate by magnetron sputtering under ultrahigh vacuum conditions. The lattice parameters of Fe ($d^0_{\mathrm{Fe}} = 2.87$ Å) and V ($d^0_{\mathrm{V}} = 3.03$ Å) are close enough to allow epitaxial growth on suitable substrates, such as MgO [36]. The difference in the lattice parameter of the constituents is used to obtain close to perfect matching to the substrate [2.98 Å $= (4.211/\sqrt{2})$ Å], by the choice of the Fe to V ratio. The in-plane lattice parameter of both Fe and V are the same (2.98 Å). The investigated samples consisted of $[\mathrm{Fe}_1/\mathrm{V}_7]_{25}$, $[\mathrm{Fe}_3/\mathrm{V}_{16}]_{25}$, and $[\mathrm{Fe}_3/\mathrm{V}_{21}]_{25}$, where the number outside the brackets refers to the number of repeats of the bilayers, and the subscripts signify the average number of atomic layers of each material. The nominal strain in the respective vanadium layers was confirmed with the measurement prescription in [37] for two of the superlattices, and a detailed discussion of the structural quality of the $[\mathrm{Fe}_1/\mathrm{V}_7]_{25}$ sample is found in Ref. [35]. A 5 nm Pd layer is used to protect the samples from oxidation and catalyze the hydrogen absorption or desorption.

The hydrogen uptake of the samples was determined in a chamber reaching a base pressure of 5×10^{-9} mbar, using a silica tube surrounded by a heating jacket (300–570 K), in the pressure range 1–10^5 Pa. The external hydrogen pressure p_{H_2} was monitored by two pressure gauges (0–133 Pa, 0–133 kPa) as described in Ref. [38]. The isotherms were determined by extracting the hydrogen concentration from the optical transmittance at 639 nm for preset temperatures and pressures. The onset of ordering of hydrogen as well as the point when the sample had reached equilibrium with the gas phase was obtained from simultaneous resistivity measurements as described in Ref. [38]. The resistivity consistently returned to the prehydrogenated values which allowed us to conclude that no irreversible changes occurred during the hydrogen absorption or desorption process. Figure 2 depicts representative p-c-T isotherms. The coefficient used to convert the changes in optical transmission to concentration is obtained from a combination of neutron scattering [39] and optical measurements on a $((\mathrm{Fe}_{0.5}\mathrm{V}_{0.5})_6/\mathrm{V}_{21}$ superlattice.

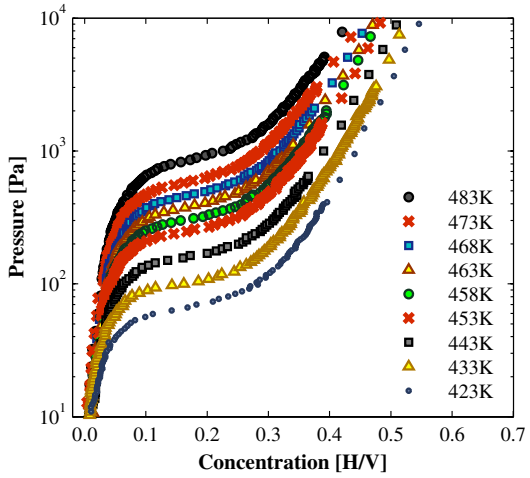

FIG. 2 (color online). Pressure-composition isotherms of hydrogen in the V layers for the $\mathrm{Fe}_3/\mathrm{V}_{16}$ sample. The concentration is in units of atomic ratio.

In order to quantify the finite-size dependence of the phase transition, the spinodal (T_{sp}) and critical (T_{crit}) temperatures were extracted in the following way: First, the chemical potential, $\mu - \mu_0 = k_B T \ln(p/p_0)$, with μ_0 the standard chemical potential, was determined from the applied hydrogen pressure (p), using 1 bar as a reference ($p_0 = 10^5$ Pa). This equation relates the pressure of the external hydrogen to the chemical potential of hydrogen in the metal hydride [27]. Thereafter, we plot the chemical potential versus temperature for all concentrations (van't Hoff plot) [27], as shown in Fig. 3. The derivative of the

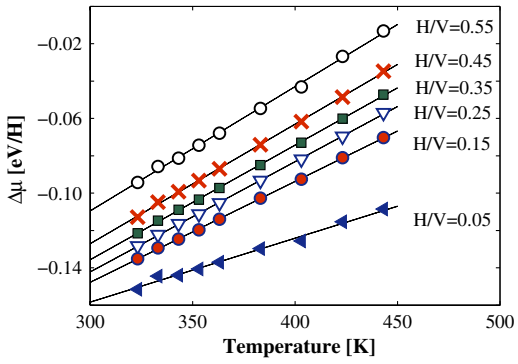

FIG. 3 (color online). Representative changes in the chemical potential as a function of temperature for the $\mathrm{Fe}_1/\mathrm{V}_7$ sample.

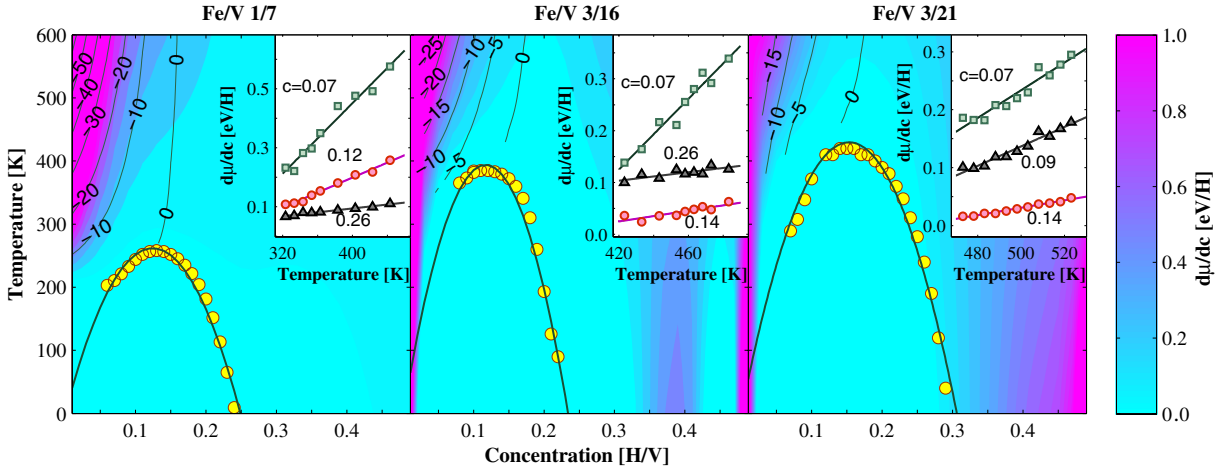

FIG. 4 (color online). Changes in the chemical potential with respect to hydrogen concentration as a function of temperature and concentration are shown as a color map. The solid lines are isolines of the second derivative of the chemical potential with respect to concentration. The yellow circles follow from the Curie-Weiss analysis and mark the spinodal temperature. Note that $\Delta\mu$ below 320 K is extracted based on an extrapolation of the linear fit of the van't Hoff plot. The solid line represents a fit to the spinodal line. The insets in the figures depict the Curie Weiss analysis. Note that all phase diagrams were measured at the same strain values in the vanadium layers.

chemical potential with respect to concentration is plotted in Fig. 4 versus concentration and temperature. The insets in Fig. 4 show that the derivative of the chemical potential of hydrogen with respect to concentration can be described by the Curie-Weiss law. This demonstrates that any temperature dependence of the entropy must be small [40]. The spinodal and critical temperatures can be obtained from the measured slope of the chemical potential isotherms for each concentration at the point when $(\partial\mu/\partial c) = 0$ (marked by the circles in the three panels of Fig. 4).

By evaluating the equation of state, including the configurational entropy [27], $\mu = -uc + kT\ln[c/(r-c)]$, the spinodal temperature can be linked to the (pairwise) H-H interaction u, the concentration of hydrogen c, and the blocking parameter or maximum concentration r:

$$T_{\mathrm{sp}} = \frac{uc(r-c)}{k_B r}. \qquad (1)$$

Excellent agreement between Eq. (1) and the extrapolated experimental data is found (see Fig. 4), although we have neglected the entropy contributions from acoustic, optical, volume, and electronic sources. The critical temperature T_{crit} can be extracted from the fit of the spinodal line. This leads to a direct link of the critical concentration and the blocking parameter, $c_{\mathrm{crit}} = (r/2)$. The extracted values for T_{crit}, u, and c_{crit} are summarized in Table I.

TABLE I. Obtained fitting results.

Sample		Fe_1V_7	Fe_3V_{16}	Fe_3V_{21}
Critical concentration:	c_{crit} [H/V]	0.12(1)	0.12(1)	0.15(1)
H-H interaction:	u [eV]	0.36(2)	0.59(2)	0.48(2)
Critical temperature:	T_{crit} [K]	252(22)	403(17)	445(11)

The critical concentrations are smaller than previously obtained for bulk (0.25 H/V [41]). Furthermore, the H-H interaction (Table I) is considerably larger than that obtained for bulk vanadium (0.2 eV [27]). These findings are in line with earlier measurements and calculations on tetragonally distorted vanadium films [30,33]. The strength of the H-H interaction was determined using the concentration dependence of the enthalpy ΔH, obtained by van't Hoff analysis of the isotherms (see inset in Fig. 5). At low concentrations the slope, i.e., the H-H interaction $(u = (\partial\Delta H/\partial c))$, is substantially larger in the strained V layers than for bulk, in line with the results above. The enhanced interaction energy is a direct consequence of the polarization of the local strain field [35], as defined by

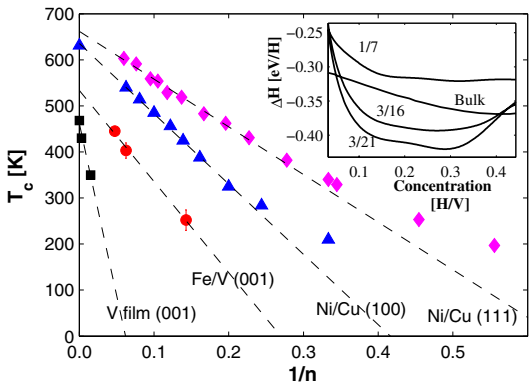

FIG. 5 (color online). The figure illustrates the inverse thickness dependence of the ordering temperature for hydrogen in ultrathin biaxially strained V lattices [Fe/V(001) superlattices (present work)], thin V layers, and the magnetic ordering temperature of Ni on Cu(001) and Cu(111) [1]. The dashed lines are fits using Eq. (2). n is the number of atomic layers.

Alefeld [8]. In the limit of zero concentration the enthalpy is independent of thickness in the V layers and finite-size effects are therefore not apparent at the lowest concentrations. This is expected, as finite-size effects arise from the changes in interaction in the direction perpendicular to the surface of the confined layers.

When addressing finite-size effects upon hydrogen absorption, the presence of depletion regions near surfaces and interfaces needs to be taken into account [39,42,43]. To accomplish this we use a simple model based upon missing (H-H) neighbors at the Fe/V interfaces [42], analogous to the interface effects in magnetic layers [9]:

$$T_{\mathrm{crit}} = T_{\mathrm{crit},\infty}\left(1 - \frac{1 + 2\Delta n}{n}\right). \quad (2)$$

Here, $T_{\mathrm{crit},\infty}$ denotes the critical temperature extrapolated for an infinitely thick strained film, n is the number of vanadium layers, and Δn is the thickness of the depleted layers, assuming these to be hydrogen free. The change in the critical temperature (Table I) with inverse thickness of the V(001) layers is shown in Fig. 5. The critical temperatures for 10 and 50 nm films are included for comparison [44] as well as the magnetic ordering temperature of Ni on Cu(100) and Cu(111) [1]. Using this representation highlights two important features: $T_{\mathrm{crit},\infty}$ follows directly from the linear extrapolation to infinite sample thicknesses and the extension of the interface regions can be extracted at $T_{\mathrm{crit}} = 0$. The dashed lines represent fits to the data using the equation above with $\Delta n = 1.4^{+0.6}_{-0.1}$ and $T_{\mathrm{crit},\infty} = 533^{+46}_{-13}$ K. The obtained $T_{\mathrm{crit},\infty}$ is larger than the value reported for bulk and thin films (see Fig. 5), which is a direct result of the imposed polarization of the strain field, increasing the effective H-H interaction [34]. In the thick film limit, the scaling of the magnetic ordering temperature with inverse thickness holds well for Ni on both Cu(111) and Cu(100), while the extrapolated $T_{\mathrm{crit},\infty}$ displays similar shifts as observed for H in the thin V layers. The root of this shift is not known, but a contribution from strain induced magnetic anisotropy is most likely of importance. We also note the changes in the slope in the few monolayer limit, which can be argued to arise from the changes in the strain state of Ni, are caused by the nonideal lattice matching between Ni and Cu.

We therefore conclude that the critical temperature of hydride formation scales inversely with the layer thickness and that profound finite-size effects are only observed on the nm length scale. As a consequence, one would not expect ordering for H absorbed in a single monolayer of vanadium. These results are directly comparable to the thickness dependence of magnetic properties [1,2], where a suppression of the critical temperature is found. The results can also be related to surface and interface effects in ice where premelting at the surface is reported [6,7]. The results, therefore, add an important angle to the generality of the influence of extension on thermodynamic behavior. The results also have important implications with respect to the use of hydrogen as an energy carrier: Phase transitions in metal hydride systems can be suppressed by tuning of the critical temperature via a change in thickness. This implies a possible route for reversible charging and discharging, completely avoiding hydrogen induced embrittlement in wide temperature and concentration ranges. The results also unambiguously demonstrate that nanometer-sized materials are needed to exploit real finite-size effects.

*max.wolff@physics.uu.se

[1] F. Huang, M. T. Kief, G. J. Mankey, and R. F. Willis, Phys. Rev. B **49**, 3962 (1994).
[2] E. Weschke *et al.*, Phys. Rev. Lett. **93**, 157204 (2004).
[3] M. Ahlberg, M. Marcellini, A. Taroni, G. Andersson, M. Wolff, and B. Hjörvarsson, Phys. Rev. B **81**, 214429 (2010).
[4] V. Leiner, K. Westerholt, A. M. Blixt, H. Zabel, and B. Hjörvarsson, Phys. Rev. Lett. **91**, 037202 (2003).
[5] T. Li, D. Donadio, and G. Galli, Nat. Commun. **4**, 1887 (2013).
[6] R. Rosenberg, Phys. Today **58**, No. 12, 50 (2005).
[7] Y. Li and G. A. Somorjai, J. Phys. Chem. C **111**, 9631 (2007).
[8] G. Alefeld, Ber. Bunsen-Ges. Phys. Chem. **76**, 746 (1972), http://onlinelibrary.wiley.com/doi/10.1002/bbpc.19720760809/abstract.
[9] A. Taroni and B. Hjörvarsson, Eur. Phys. J. B **77**, 367 (2010).
[10] H. Zabel and H. Peisl, Phys. Rev. Lett. **42**, 511 (1979).
[11] E. Tal-Gutelmacher, A. Pundt, and R. Kirchheim, J. Mater. Sci. **45**, 6389 (2010).
[12] G. Song, M. Geitz, A. Abromeit, and H. Zabel, Phys. Rev. B **54**, 14093 (1996).
[13] A. Remhof and A. Borgschulte, ChemPhysChem **9**, 2440 (2008).
[14] A. Pundt, Adv. Eng. Mater. **6**, 11 (2004).
[15] A. Pundt and R. Kirchheim, Annu. Rev. Mater. Res. **36**, 555 (2006).
[16] J. Weissmuller and C. Lemier, Philos. Mag. Lett. **80**, 411 (2000).
[17] P. E. de Jongh and P. Adelhelm, ChemSusChem **3**, 1332 (2010).
[18] T. K. Nielsen, F. Besenbacher, and T. R. Jensen, Nanoscale **3**, 2086 (2011).
[19] A. Baldi and B. Dam, J. Mater. Chem. **21**, 4021 (2011).
[20] G. K. Pálsson, A. Bliersbach, M. Wolff, A. Zamani, and B. Hjörvarsson, Nat. Commun. **3**, 892 (2012).
[21] S.-i. Orimo, Y. Nakamori, J. R. Eliseo, A. Züttel, and C. J. Jensen, Chem. Rev. **107**, 4111 (2007).
[22] I. P. Jain, P. Jain, and A. Jain, J. Alloys Compd. **503**, 303 (2010).
[23] B. Sakintuna, F. Lamari-Darkrim, and M. Hirscher, Int. J. Hydrogen Energy **32**, 1121 (2007).
[24] J.-F. Herbst and L. G. Hector Jr., Appl. Phys. Lett. **88**, 231904 (2006).
[25] L. Schlapbach and A. Zuttel, Nature (London) **414**, 353 (2001).
[26] T. Schober and H. Wenzl, *Hydrogen in Metals II* (Springer, Berlin, Heidelberg, 1978), Vol. 29, p. 11.

[27] Y. Fukai, *The Metal-Hydrogen System: Basic Bulk Properties*, Springer Series in Materials Science Series (Springer-Verlag Berlin, Heidelberg, 2005).
[28] H. Bleichert and H. Wenzl, Phys. Status Solidi B **144**, 361 (1987).
[29] R. Griessen and T. Riesterer, *Hydrogen in Intermetallic Compounds I*, Topics in Applied Physics (Springer, New York, 1988), Vol. 63.
[30] G. Andersson, P. H. Andersson, and B. Hjörvarsson, J. Phys. Condens. Matter **11**, 6669 (1999).
[31] B. Hjörvarsson, G. Andersson, and E. Karlsson, J. Alloys Compd. **253–254**, 51 (1997).
[32] G. Reynaldsson, S. Ólafsson, and H. Gislason, J. Alloys Compd. **356–357**, 545 (2003).
[33] G. K. Pálsson, M. Wälde, M. Amft, Y. Wu, M. Ahlberg, M. Wolff, A. Pundt, and B. Hjörvarsson, Phys. Rev. B **85**, 195407 (2012).
[34] S. Olsson, A. Blixt, and B. Hjörvarsson, J. Phys. Condens. Matter **17**, 2073 (2005).
[35] G. K. Pálsson, A. R. Rennie, and B. Hjörvarsson, Phys. Rev. B **78**, 104118 (2008).
[36] P. Isberg, B. Hjörvarsson, R. Wäppling, E. B. Svedberg, and L. Hultman, Vacuum **48**, 483 (1997).
[37] J. Birch, J.-E. Sundgren, and P. Fewster, J. Appl. Phys. **78**, 6562 (1995).
[38] J. Prinz, G. K. Pálsson, P. T. Korelis, and B. Hjörvarsson, Appl. Phys. Lett. **97**, 251910 (2010).
[39] G. K. Pálsson, V. Kapaklis, J. A. Dura, J. Jacob, S. Jayanetti, A. R. Rennie, and B. Hjörvarsson, Phys. Rev. B **82**, 245424 (2010).
[40] H. Horner and H. Wagner, J. Phys. C **7**, 3305 (1974).
[41] E. Veleckis and R. K. Edwards, J. Phys. Chem. **73**, 683 (1969).
[42] B. Hjörvarsson, J. Ryden, E. Karlsson, J. Birch, and J.-E. Sundgren, Phys. Rev. B **43**, 6440 (1991).
[43] V. Meded and S. Mirbt, Phys. Rev. B **71**, 024207 (2005).
[44] J. Bloch, B. Pejova, J. Jacob, and B. Hjörvarsson, Phys. Rev. B **82**, 245428 (2010).